THE ASTRONOMICAL JOURNAL, 120:1085–1099, 2000 August

NEW NEIGHBORS FROM 2MASS: ACTIVITY AND KINEMATICS AT THE BOTTOM OF THE MAIN SEQUENCE

JOHN E. GIZIS[1]
Infrared Processing and Analysis Center, 100-22, California Institute of Technology, Pasadena, CA 91125; gizis@ipac.caltech.edu
DAVID G. MONET[1]
US Naval Observatory, P.O. Box 1149, Flagstaff, AZ 86002
I. NEILL REID
Department of Physics and Astronomy, University of Pennsylvania, 209 South 33rd Street, Philadelphia, PA 19104-6396
J. DAVY KIRKPATRICK
Infrared Processing and Analysis Center, 100-22, California Institute of Technology, Pasadena, CA 91125
JAMES LIEBERT
Steward Observatory, University of Arizona, Tucson, AZ 85721
AND
RIK J. WILLIAMS
Department of Astronomy, MSC 152, California Institute of Technology, Pasadena, CA 91126-0152
Received 2000 February 1; accepted 2000 April 26

ABSTRACT

We have combined 2MASS and POSS II data in a search for nearby ultracool (later than M6.5) dwarfs with $K_s < 12$. Spectroscopic follow-up observations identify 53 M7–M9.5 dwarfs and seven L dwarfs. The observed space density is 0.0045 ± 0.0008 M8–M9.5 dwarfs per cubic parsec, without accounting for biases, consistent with a mass function that is smooth across the stellar/substellar limit. We show the observed frequency of Hα emission peaks at $\sim$100% for M7 dwarfs and then decreases for cooler dwarfs. In absolute terms, however, as measured by the ratio of Hα to bolometric luminosity, none of the ultracool M dwarfs can be considered very active compared to earlier M dwarfs, and we show that the decrease that begins at spectral type M6 continues to the latest L dwarfs. We find that flaring is common among the coolest M dwarfs and estimate the frequency of flares at 7% or higher. We show that the kinematics of relatively active (EW > 6 Å) ultracool M dwarfs are consistent with an ordinary old disk stellar population, while the kinematics of inactive ultracool M dwarfs are more typical of a 0.5 Gyr old population. The early L dwarfs in the sample have kinematics consistent with old ages, suggesting that the hydrogen-burning limit is near spectral types L2–L4. We use the available data on M and L dwarfs to show that chromospheric activity drops with decreasing mass and temperature and that at a given (M8 or later) spectral type, the younger field (brown) dwarfs are less active than many of the older, more massive field stellar dwarfs. Thus, contrary to the well-known stellar age-activity relationship, low activity in field ultracool dwarfs can be an indication of comparative youth and substellar mass.

Key words: solar neighborhood — stars: activity — stars: kinematics — stars: low-mass, brown dwarfs — stars: luminosity function, mass function

1. INTRODUCTION

Catalogs of nearby stars (Gliese & Jahreiss 1991; Kirkpatrick, Henry, & Simons 1995; Reid, Hawley, & Gizis 1995) and high proper-motion stars (Luyten 1979) are grossly deficient in very low mass (VLM) dwarfs. With spectral types of M7 and later, these objects, sometimes called "ultracool M dwarfs,"[2] are so optically faint that even nearby ones eluded searches based on the older (pre-1980s) sky surveys. These dwarfs have particular importance because they lie at or below the hydrogen-burning limit and have proved not only to be estimators of the numbers of dark brown dwarfs but also present interesting astrophysical challenges in their own right.

The new generation of sky surveys allows this deficiency to be addressed and large samples of nearby VLM dwarfs to be identified. The Two Micron All-Sky Survey[3] (M. F. Skrutskie et al., in preparation, hereafter 2MASS) provides reliable photometry in the JHK_s passbands, close to the peak of emission for these cool dwarfs. Furthermore, the Second Palomar Sky Survey (Reid et al. 1991, hereafter POSS II) provides B_J, R_F, and I_N photographic photometry in the northern hemisphere. In the southern hemisphere, the UK Schmidt and ESO sky survey plates provide B_J and R_F magnitudes. In sum, it is becoming possible to identify both the least luminous stars and young massive brown dwarfs by their optical and near-infrared colors alone over most of the sky.

[1] Visiting Astronomer, Kitt Peak National Observatory, National Optical Astronomy Observatories, which is operated by the Association of Universities for Research in Astronomy, Inc. (AURA) under cooperative agreement with the National Science Foundation.

[2] All spectral types in this paper are on the Kirkpatrick, Henry, & McCarthy (1991) M dwarf and Kirkpatrick et al. (1999b) L dwarf systems. L dwarfs are cooler than "ultracool" M dwarfs.

[3] 2MASS data and documentation are available at http://www.ipac.caltech.edu/2mass.

We present first results of a search using near-infrared and optical sky survey data aimed at completing the nearby star catalog for the ultracool M dwarfs. We discuss the sample selection and spectroscopic follow-up in § 2. Although the sample discussed in this paper includes only a small fraction of the total population of nearby ultracool dwarfs, it represents a fourfold increase in the number of such sources known. We discuss some preliminary results concerning the statistical properties of these sources in the latter sections of this paper. We discuss some stars of special interest in § 3 and the 2MASS colors of ultracool M dwarfs in § 4. The local space density of VLM dwarfs is discussed in § 5, their activity and kinematics are discussed in § 6, and finally our conclusions and future prospects are discussed in § 7.

2. DATA

2.1. *Sample Selection*

Our results are based on three observational samples. For our initial observing run, in 1998 July, we used both photometric and proper-motion criteria to define a sample of candidate VLM dwarfs. Based on the results from this run and further experience analyzing 2MASS data, we were able to improve our selection criteria for our 1998 December and subsequent observing runs. There are thus three samples with different properties, and when necessary we distinguish them as "Sample A" (1998 July), "Sample B" (1998 December), and "Sample C" (1999 June), respectively. Samples B and C have nearly identical selection criteria and when combined are referred to as Sample BC. In all samples, objects within 20° of the Galactic plane were excluded. Unless otherwise stated, all the analysis in §§ 5 and 6 is based on Sample BC. Table 1 lists all the targets.

Sample A was based on 2MASS data processed by 1998 July. All these data were obtained at the Mount Hopkins 2MASS telescope, and a total of 363 deg^2 were searched. All objects classified as extended by the 2MASS pipeline were eliminated (Jarrett et al. 2000). The 2MASS data were correlated with the USNO's PMM scans of the POSS II plates, using a preliminary version of the software used by the 2MASS Rare Objects Core Project (this software will be described in more detail in a future publication by Monet et al.). This provided three additional colors: B_J, R_F, and I_N. Zero-point calibrations for the POSS II scans were not available, but we have since found that rough zero points (good to ± 0.5 mag) are $B = B_{J\mathrm{inst}} + 2$, $R_C = R_{F\mathrm{inst}} - 1$, and $I_C = I_{N\mathrm{inst}} - 1$ (Gizis, Reid, & Monet 1999). These do not account for plate-to-plate variations or the significant color terms expected in B_J and R_F.

All objects that met the following criteria were observed:

1. $9.0 \leq K_s \leq 13.0$.
2. $0.95 \leq J-K_s < 1.30$.
3. No B_J detection.
4. Significant ($>2\,\sigma$) proper motion.

Objects were also observed if they satisfied the following:

1. $9 \leq K_s \leq 12.0$.
2. $0.95 \leq J-K_s < 1.30$.
3. B_J detection.
4. Significant ($>2\,\sigma$) proper motion.

The proper-motion criterion requires elaboration. The magnitude of the observed positional offset between the 2MASS and POSS II source is compared to the distribution of all 2MASS–POSS II correlations. Only objects with significant proper motion were selected. Thus, while we selected sources that are moving with high confidence (roughly 2 σ), the actual cutoff in terms of arcseconds per year depends on the epoch difference between the F plate and 2MASS, which varies between 0 and ~ 10 yr.

As shown in § 2.2, these criteria led to the identification of a number of new nearby M dwarfs, but they are flawed in some respects. First, the POSS II and UKST IIIa J plates are sufficiently sensitive that many nearby (bright) VLM dwarfs are detected. Moreover, the blue cutoff in $J-K_s$ allowed mid-M dwarfs to enter the sample. We selected this blue cutoff because the prototypical M7 dwarf VB 8 has $J-K = 0.95$ (Leggett 1992). However, M dwarfs between spectral type M0 and M6.5 all have $J-K_s \approx 0.9$, and, with uncertainties of $\sigma_{J-K} \approx 0.04$ mag, significant numbers are scattered to $J-K_s > 0.95$. Consequently, our initial attempts to select ultracool M dwarfs produced a sample that is heavily contaminated by distant mid-M dwarfs. As it turned out, there were no 2MASS sources meeting our color and magnitude cuts that were not paired with a POSS II source in Sample A.

Based on experience gained from this analysis, we revised our sample selection for the 1998 December observing run. Because a larger area was available, we focused on brighter VLM dwarfs which should lie within ~ 20 pc. The Sample B criteria are as follows:

1. $K_s \leq 12.0$.
2. $J-K_s \geq 1.00$.
3. $R_F-K_s > 3.5$ or $I_N-K_s \geq 2.0$.
4. $\delta < +30°$.
5. $\alpha < 13^{\mathrm{h}}00^{\mathrm{m}}$ or $\alpha > 20^{\mathrm{h}}00^{\mathrm{m}}$.
6. $J-H \leq (4/3)H-K + 0.25$.

No selection based on proper motion was applied, and therefore Sample B is kinematically unbiased. A total of 2977 deg^2 were searched. The $J-K_s$ cutoff excludes early and mid-M dwarfs but also some of the bluer M7 dwarfs. Nearby bright L dwarfs, however, are included in these samples, since we impose no red cutoff. Both samples are magnitude selected and therefore are biased toward overluminous stars and unresolved near-equal luminosity binaries, although binaries with separations of a few arcseconds may be excluded by the extended source provision. The position selection is due to the requirement that the objects be observable from Las Campanas in December. Ultracool M dwarfs have $R-K_s > 5.5$ and $I-K > 3.4$ (Leggett 1992), but we used a more liberal selection to allow for uncertainties in the calibration of the photographic magnitudes. In § 4, we show that $R-K_s > 4.9$ includes all M8 and later dwarfs. The $J-H$, $H-K$ cut excludes M giants.

Sample C was selected for our 1999 June Kitt Peak observing run. The selection was identical to the Sample B selection, except that a different area was covered and only objects with $R-K_s > 4.9$ were selected. Processed data that lay within the following limits were selected:

1. $\alpha > 11^{\mathrm{h}}00^{\mathrm{m}}$ and $\delta > +6°$.
2. $16^{\mathrm{h}}20^{\mathrm{m}} < \alpha < 23^{\mathrm{h}}35^{\mathrm{m}}$ and $-36° < \delta < +6°$.

2.2. *Spectroscopy and Data Analysis*

Sample A was observed on UT dates 1998 July 30–August 1 using the Double Spectrograph and the Hale 200

TABLE 1

TARGETS

Name	R.A. (J2000)	Decl. (J2000)	J	H	K_s	Sp.	Hα EW	Sample
2MASSI J0010325+171549	00:10:32.50	+17:15:49.2	13.88	13.18	12.81	M8.0	4.2	A
2MASSW J0016533+275534.....	00:16:53.37	+27:55:34.9	12.82	12.12	11.77	M6	7.2	B
2MASSW J0027559+221932[a].....	00:27:55.91	+22:19:32.9	10.61	9.97	9.56	M8.0	6.1	B
2MASSW J0036159+182110.....	00:36:15.98	+18:21:10.2	12.44	11.56	11.02	L3.5	0.0	B
2MASSI J0104377+145724	01:04:37.70	+14:57:24.0	13.70	13.02	12.61	M8.0	2.9	A
2MASSI J0105190+140740	01:05:19.02	+14:07:40.9	13.59	12.92	12.55	M7.0	10.2	A
2MASSW J0109216+294925.....	01:09:21.69	+29:49:25.7	12.92	12.19	11.70	M9.5	0.0	B
2MASSW J0130058+172143.....	01:30:05.82	+17:21:43.8	13.66	12.98	12.58	M8.0	0.6	A
2MASSW J0130144+271722.....	01:30:14.46	+27:17:22.2	12.90	12.32	11.87	M6	5.2	B
2MASSW J0140026+270150.....	01:40:02.64	+27:01:50.6	12.51	11.82	11.44	M8.5	0.0	B
2MASSI J0149089+295613	01:49:08.96	+29:56:13.2	13.41	12.55	11.99	M9.5	11.0	B
2MASSI J0218591+145116	02:18:59.13	+14:51:16.2	14.18	13.58	13.25	M7.0	6.0	A
2MASSI J0220181+241804	02:20:18.16	+24:18:04.9	13.01	12.32	11.91	M6	5.0	B
2MASSI J0240295+283257	02:40:29.51	+28:32:57.6	12.62	11.99	11.62	M7.5	8.4	B
2MASSI J0253202+271333	02:53:20.28	+27:13:33.2	12.49	11.82	11.45	M8.0	16.0	B
LP 412-31	03:20:59.65	+18:54:23.3	11.74	11.04	10.57	M9.0	29.0	B
2MASSI J0330050+240528[b]	03:30:05.07	+24:05:28.3	12.36	11.75	11.36	M7.0	30.7	B
2MASSI J0335020+234235	03:35:02.08	+23:42:35.6	12.26	11.65	11.26	M8.5	4.6	B
2MASSW J0350573+181806[c].....	03:50:57.36	+18:18:06.5	12.95	12.22	11.76	M9.0	0.0	B
2MASSW J0354013+231633.....	03:54:01.34	+23:16:33.9	13.12	12.42	11.97	M8.5	6.8	B
LP 415-20	04:21:49.56	+19:29:08.6	12.68	12.04	11.65	M7.5	4.4	B
LP 475-855	04:29:02.83	+13:37:59.2	12.67	11.98	11.64	M7.0	40.5	B
2MASSI J0746425+200032	07:46:42.56	+20:00:32.2	11.74	11.00	10.49	L0.5	0.0	B
2MASSI J0810586+142039	08:10:58.65	+14:20:39.1	12.71	12.04	11.61	M9.0	6.1	B
2MASSI J0818580+233352	08:18:58.05	+23:33:52.2	12.14	11.50	11.13	M7.0	9.5	B
2MASSI J0925348+170441[d]	09:25:34.85	+17:04:41.5	12.60	11.99	11.60	M7.0	4.7	B
2MASSW J0952219−192431.....	09:52:21.91	−19:24:31.8	11.88	11.28	10.85	M7.0	9.3	B
LHS 2243	10:16:34.70	+27:51:49.8	11.95	11.29	10.95	M7.5	43.8	B
2MASSI J1024099+181553	10:24:09.98	+18:15:53.4	12.24	11.58	11.21	M7.0	4.4	B
2MASSW J1049414+253852.....	10:49:41.44	+25:38:52.9	12.40	11.75	11.39	M6	6.9	B
2MASSW J1108307+683017.....	11:08:30.79	+68:30:17.1	13.14	12.23	11.60	L1	7.8	C
LHS 2397a	11:21:49.25	−13:13:08.5	11.93	11.26	10.72	M8.5	15.3	B
2MASSW J1127534+741107.....	11:27:53.48	+74:11:07.9	13.06	12.37	11.97	M8.0	3.0	C
2MASSW J1200329+204851.....	12:00:32.92	+20:48:51.3	12.85	12.25	11.82	M7.0	3.9	C
BRI 1222−1221	12:24:52.21	−12:38:35.3	12.56	11.83	11.37	M9.0	4.7	B
2MASSW J1237270−211748.....	12:37:27.05	−21:17:48.1	12.67	12.05	11.64	M6	8.3	B
LHS 2632.....	12:46:51.72	+31:48:11.1	12.26	11.59	11.23	M6.5	0.0	C
2MASSW J1300425+191235.....	13:00:42.55	+19:12:35.6	12.71	12.07	11.61	L1	0.0	C
2MASSW J1311391+803222.....	13:11:39.16	+80:32:22.2	12.81	12.14	11.71	M8.0	3.0	C
2MASSW J1336504+475131.....	13:36:50.46	+47:51:31.9	12.64	12.06	11.63	M7.0	5.0	C
2MASSW J1344582+771551.....	13:44:58.24	+77:15:51.3	12.88	12.27	11.83	M7.0	2.7	C
2MASSW J1403223+300755.....	14:03:22.34	+30:07:55.0	12.69	12.01	11.63	M8.5	18.7	C
2MASSW J1421314+182740.....	14:21:31.44	+18:27:40.5	13.21	12.43	11.93	M9.5	3.6	C
2MASSI J1426316+155701	14:26:31.61	+15:57:01.3	12.87	12.18	11.71	M9.0	1.2	C
2MASSW J1439283+192915.....	14:39:28.37	+19:29:15.0	12.76	12.05	11.58	L1	0.0	C
2MASSW J1444171+300214[e].....	14:44:17.17	+30:02:14.3	11.68	10.97	10.57	M8.0	7.4	C
2MASSW J1457396+451716.....	14:57:39.66	+45:17:16.8	13.14	12.41	11.92	M9.0	5.5	C
2MASSW J1506544+132106.....	15:06:54.40	+13:21:06.0	13.41	12.41	11.75	L3	1.0	C
2MASSW J1543581+320642[f].....	15:43:58.14	+32:06:42.0	12.73	12.12	11.73	M6.5	5.2	C
2MASSW J1546054+374946.....	15:46:05.40	+37:49:46.1	12.44	11.79	11.42	M7.5	10.9	C
2MASSW J1550381+304103.....	15:50:38.19	+30:41:03.7	12.99	12.41	11.92	M7.5	13.7	C
2MASSW J1551066+645704.....	15:51:06.63	+64:57:04.6	12.87	12.15	11.73	M8.5	11.5	C
2MASSW J1553199+140033.....	15:53:19.93	+14:00:33.8	13.02	12.27	11.85	M9.0	8.7	C
2MASSW J1627279+810507.....	16:27:27.93	+81:05:07.9	13.04	12.33	11.87	M9.0	6.1	C
2MASSW J1635192+422305.....	16:35:19.20	+42:23:05.4	12.89	12.21	11.80	M8.0	2.1	C
2MASSW J1658037+702701.....	16:58:03.77	+70:27:01.7	13.31	12.54	11.92	L1	0.0	C
2MASSW J1707183+643933.....	17:07:18.31	+64:39:33.4	12.56	11.83	11.39	M9.0	9.8	C
2MASSW J1714523+301941.....	17:14:52.34	+30:19:41.0	12.94	12.28	11.89	M6.5	5.4	C
2MASSW J1733189+463359.....	17:33:18.92	+46:33:59.6	13.21	12.41	11.86	M9.5	2.4	C
2MASSW J1750129+442404.....	17:50:12.90	+44:24:04.5	12.79	12.17	11.76	M7.5	2.7	C
2MASSW J1757154+704201[g].....	17:57:15.40	+70:42:01.1	11.45	10.84	10.37	M7.5	3.0	C
2MASSW J2013510−313651.....	20:13:51.02	−31:36:51.3	12.67	12.06	11.67	M6	6.2	C
LHS 3566.....	20:39:23.81	−29:26:33.4	11.35	10.77	10.35	M6	0.0	C
2MASSW J2049197−194432.....	20:49:19.74	−19:44:32.5	12.87	12.24	11.77	M7.5	13.1	C
2MASSW J2052086−231809[h].....	20:52:08.61	−23:18:09.6	12.26	11.62	11.26	M6.5	5.8	C

TABLE 1—*Continued*

Name	R.A. (J2000)	Decl. (J2000)	J	H	K_s	Sp.	Hα EW	Sample
2MASSW J2113029−100941	21:13:02.94	−10:09:41.0	12.86	12.22	11.81	M6	0.0	C
2MASSW J2135146−315345	21:35:14.65	−31:53:45.9	12.81	12.12	11.76	M6	7.6	C
2MASSW J2140293+162518	21:40:29.32	+16:25:18.4	12.94	12.27	11.78	M8.5	0.0	C
2MASSI J2147436+143131	21:47:43.66	+14:31:31.8	13.84	13.13	12.65	M8.0	3.3	A
2MASSW J2147446−264406	21:47:44.62	−26:44:06.6	13.04	12.37	11.92	M7.5	3.9	C
2MASSW J2202112−110946[i]	22:02:11.26	−11:09:46.0	12.36	11.71	11.36	M6.5	10.2	C
2MASSW J2206228−204705	22:06:22.80	−20:47:05.8	12.43	11.75	11.35	M8.0	5.6	B
2MASSI J2221531+115823	22:21:53.15	+11:58:23.0	13.30	12.68	12.30	M7.5	1.5	A
2MASSW J2221544+272907	22:21:54.43	+27:29:07.5	12.52	11.92	11.52	M6	3.6	B
2MASSW J2233478+354747[j]	22:33:47.85	+35:47:47.8	11.94	11.30	10.88	M6	6.6	C
2MASSI J2234138+235956	22:34:13.88	+23:59:56.1	13.14	12.33	11.81	M9.5	4.4	B
2MASSI J2235490+184029[k]	22:35:49.07	+18:40:29.8	12.46	11.83	11.33	M7.0	8.5	B
2MASSI J2255584+282246[l]	22:55:58.45	+28:22:46.7	12.55	11.94	11.54	M6	5.2	B
2MASSW J2306292−050227	23:06:29.29	−05:02:27.9	11.37	10.72	10.29	M7.5	4.9	C
2MASSW J2313472+211729[m]	23:13:47.29	+21:17:29.5	11.43	10.75	10.42	M6	6.0	B
2MASSW J2331016−040618	23:31:01.63	−04:06:18.6	12.94	12.29	11.93	M8.0	5.4	C
2MASSI J2334394+193304	23:34:39.44	+19:33:04.2	12.77	12.07	11.64	M8.0	22.6	B
2MASSI J2336439+215338[n]	23:36:43.92	+21:53:38.7	12.76	12.10	11.71	M7.0	7.7	B
2MASSW J2347368+270206	23:47:36.80	+27:02:06.8	13.19	12.45	12.00	M9.0	3.0	B
2MASSW J2349489+122438[o]	23:49:48.99	+12:24:38.8	12.62	11.95	11.56	M8.0	3.5	C
2MASSW J2358290+270205[p]	23:58:29.00	+27:02:05.5	12.71	12.05	11.68	M6	5.9	B

[a] LP 349-25.
[b] LP 356-770.
[c] LP 413-53.
[d] LP 427-38.
[e] LP 326-21.
[f] LP 328-36.
[g] LP 44-162.
[h] LP 872-22.
[i] LP 759-17.
[j] LP 288-31.
[k] LP 460-44.
[l] LP 345-18.
[m] LP 461-11.
[n] LP 402-58.
[o] LP 523-55.
[p] LP 348-11.

inch (5 m) telescope during an observing run that was primarily devoted to our ongoing spectroscopic survey of Luyten high proper-motion stars (Gizis & Reid 1997). The wavelength coverage included 6290–8800 Å at a resolution of 3 Å.

Sample B was observed on 1998 December 2–7 using the Modular Spectrograph on the Las Campanas 100 inch (2.5 m) telescope. The "Tek 5" chip, a 2048 square CCD with 24μ pixels, was used with a 600 line mm^{-1} grating blazed at 7500 Å. The useful wavelength range of the spectra was 6100–9400 Å at a resolution of 6 Å. A few targets (including all three objects with $J-K_s > 1.3$, which had been previously identified as L dwarf candidates) were observed during Keck observing runs (see Kirkpatrick et al. 1999b, hereafter K99, and Kirkpatrick et al. 2000, hereafter K00) using LRIS (Oke et al. 1995). The resolution was 9 Å with wavelength coverage from 6300 to 10100 Å. Observations of the flare dwarf 2MASSI J0149089+295613 have already been described in Liebert et al. (1999). The Hα activity levels adopted here are the average quiescent values. The known object BRI 1222−1222 was not observed, and we rely on the spectroscopic observations reported by Kirkpatrick et al. (1995) and Tinney & Reid (1998, hereafter TR). 2MASSW J0354013+231633 has been previously published as 2MASP J0354012+231635 (Kirkpatrick, Beichman, & Skrutskie 1997), but the spectral observations presented here are independent.

Sample C was observed 1999 June 22–23using the Ritchey-Chrétien spectrograph and the Kitt Peak 4 m telescope. The wavelength coverage was 6140 to 9200 Å using the 2048 CCD, but the extreme ends of the spectra were out of focus. A few objects were observed at the Palomar 200 inch telescope in 1999 May. The four new L dwarfs identified with the Kitt Peak data were reobserved at higher signal-to-noise ratio using Keck in 1998 July. The spectral measurements used for classification on the K99 system are given in Table 2.

All spectra were extracted and flux calibrated using IRAF. M dwarf spectral types were measured by overplotting dwarfs of known spectral type and should be good to ± 0.5 subclasses. All L dwarfs have Keck observations and were classified as in K99 and K00. A few M dwarfs in Table 1 have classifications that differ by 0.5 subclasses from previously published values—we leave our values unaltered as representative of our uncertainties. Hα fluxes were measured assuming the data were photometric (there

TABLE 2

L Dwarf Data

Name	CrH-a	Rb-b/TiO-b	Cs-a/VO-b	K I Fit	Type
2MASSW J1108307+683017.....	1.27(0−1)	0.88(1)	0.84(1)	(0)	L1 V
2MASSW J1300425+191235.....	1.53(2)	0.81(1)	0.81(0−1)	(1)	L1 V
2MASSW J1506544+132106.....	1.44(1−2)	1.18(3)	1.13(3)	(3)	L3 V
2MASSW J1658037+702701.....	1.26(0−1)	0.79(1)	0.81(0−1)	(2)	L1 V

TABLE 3

KINEMATICS AND ACTIVITY

Name	$d_{\rm phot}$	μ_α	μ_δ	$V_{\rm tan}$	$\log \frac{L_{\rm H\alpha}}{L_{\rm bol}}$
BR 1222-1221	16.6	−0.262	−0.187	25	−4.70
LHS 2243	16.6	−0.158	−0.461	38	−3.57
LHS 2397a	12.0	−0.509	−0.081	29	−4.22
LP 412-31	11.7	0.349	−0.251	24	−4.45
LP 415-20	22.3	0.127	−0.036	14	−4.56
LP 475-855	22.2	0.103	−0.016	11	−3.23
2MASSW J0027559+221932	8.3	0.403	−0.172	17	−4.52
2MASSW J0036159+182110	11.1	0.837	0.104	44	...
2MASSW J0109216+294925	18.7	1.014	0.348	95	...
2MASSW J0140026+270150	19.4	0.061	−0.252	24	...
2MASSI J0149089+295613	17.4	0.207	−0.466	42	−4.62
2MASSI J0240295+283257	22.7	0.046	−0.192	21	−4.27
2MASSI J0253202+271333	20.1	0.370	0.088	36	−4.31
2MASSI J0330050+240528	20.1	0.185	−0.039	18	−3.91
2MASSI J0335020+234235	19.2	0.058	−0.043	7	−4.71
2MASSW J0350573+181806	19.9	0.189	−0.049	18	...
2MASSW J0354013+231633	22.8	−0.168	0.064	19	−4.67
2MASSI J0746425+200032	10.4	−0.358	−0.054	18	...
2MASSI J0810586+142039	20.3	−0.034	−0.128	13	−4.69
2MASSI J0818580+233352	17.9	−0.275	−0.305	35	−4.31
2MASSI J0925348+170441	22.5	−0.232	0.010	25	−4.28
2MASSW J0952219−192431	15.4	−0.077	−0.104	9	−3.96
2MASSI J1024099+181553	18.2	−0.144	−0.070	14	−4.73
2MASSW J1108307+683017	12.8	−0.226	−0.194	18	−5.44
2MASSW J1127534+741107	24.3	−0.016	−0.030	4	−4.84
2MASSW J1200329+204851	24.1	−0.159	0.232	32	−4.44
2MASSW J1300425+191235	20.3	−0.789	−1.238	141	...
2MASSW J1311391+803222	21.3	−0.068	−0.348	36	−4.86
2MASSW J1336504+475131	22.5	0.111	−0.016	12	−4.47
2MASSW J1344582+771551	23.7	0.072	−0.005	8	−4.68
2MASSW J1403223+300755	21.4	−0.788	0.042	80	−4.07
2MASSW J1421314+182740	19.6	−0.744	−0.182	71	−4.97
2MASSI J1426316+155701	20.0	0.108	−0.056	12	−5.40
2MASSW J1439283+192915	18.5	−1.245	0.392	114	...
2MASSW J1444171+300214	12.5	−0.101	−0.336	21	−4.42
2MASSW J1457396+451716	20.7	−0.191	0.100	21	−4.76
2MASSW J1506544+132106	12.1	−1.092	0.001	63	−5.72
2MASSW J1546054+374946	20.2	−0.020	−0.120	12	−3.90
2MASSW J1550381+304103	24.2	−0.112	0.107	18	−3.73
2MASSW J1551066+645704	20.6	−0.220	0.010	22	−4.39
2MASSW J1553199+140033	21.1	−0.659	0.072	66	−4.48
2MASSW J1627279+810507	21.3	−0.209	0.338	40	−4.77
2MASSW J1635192+422305	22.4	−0.073	−0.010	8	−5.12
2MASSW J1658037+702701	17.4	−0.136	−0.315	28	...
2MASSW J1707183+643933	17.1	0.226	−0.091	20	−4.49
2MASSW J1733189+463359	17.6	0.044	−0.257	22	−5.27
2MASSW J1750129+442404	23.4	−0.018	0.151	17	−4.87
2MASSW J1757154+704201	11.7	0.006	0.338	19	−4.83
2MASSW J2049197−194432	21.9	0.193	−0.260	34	−4.24
2MASSW J2140293+162518	20.7	−0.008	−0.102	10	...
2MASSW J2147446−264406	22.9	−0.054	−0.232	26	−5.04
2MASSW J2206228−204705	18.4	0.001	−0.065	6	−4.59
2MASSI J2234138+235956	17.6	0.829	−0.034	69	−4.91
2MASSI J2235490+184029	17.3	0.326	0.042	27	−4.41
2MASSW J2306292−050227	11.3	0.889	−0.420	53	−4.61
2MASSW J2331016−040618	26.3	0.401	−0.231	58	−4.72
2MASSI J2334394+193304	20.0	−0.236	−0.117	25	−4.10
2MASSI J2336439+215338	22.4	0.379	0.024	40	−4.29
2MASSW J2347368+270206	22.2	0.313	0.033	33	−5.21
2MASSW J2349489+122438	20.7	0.025	−0.189	19	−4.78

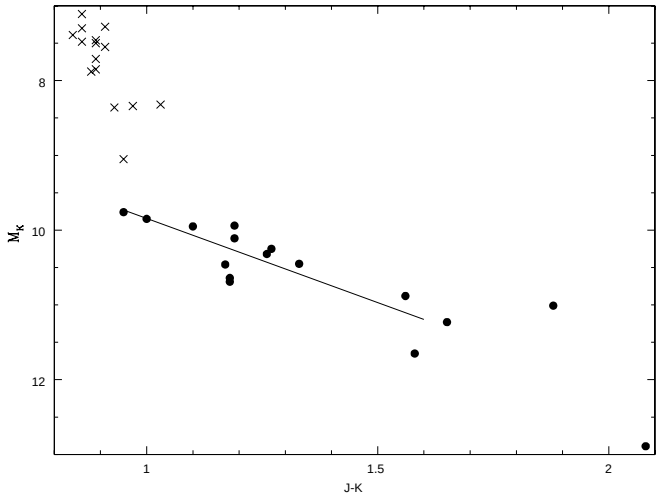

FIG. 1.—Absolute magnitudes for M7 and later dwarfs (*filled circles*) with the linear fit $M_K = 7.593 + 2.25 \times (J-K_s)$ shown. The scatter about this fit is $\sigma = 0.36$ magnitudes. 2MASS data for Hyades members from Gizis et al. (1999) are also shown to illustrate the steepness of the main sequence for M0–M7 dwarfs, which may lead to errors in the distance estimates for M7 dwarfs.

were no clouds for our observations in 1998 December). We assume that $BC_K = 3.2$ as derived by Tinney, Mould, & Reid (1993) for ultracool M dwarfs. We believe the Hα fluxes should be viewed with caution since slit losses and the high air mass of many of the observations will increase the uncertainties (the spectrograph was not adjusted to the parallactic angle). However, our derived Hα–to–bolometric luminosity ratios are consistent with those of TR, and in any case the Hα emission strength is variable in these dwarfs. In Table 3, we list our measured and derived parameters for the ultracool dwarfs in Sample BC.

Proper motions were estimated by measuring positions off the DSS (POSS *I*/UKST *J*) and XDSS (POSS II/UKST *R*) images of the photographic sky surveys. When a second epoch photographic sky survey was not available, we used the 2MASS images instead. All motions reported are relative to other stars in the field, but the correction to absolute motions is negligible compared to other sources of error in the kinematics. The proper motion reported for LHS 2397a is from Luyten (1979), and BRI 1222−1221 is from Tinney (1996). Note that all of our targets are visible on the DSS images, but most were previously unrecognized. The targets which had no POSS II pairings in our initial processing all proved to have high proper motions. They are visible on the XDSS but lie outside the 8″ search radius employed in cross-referencing against the photographic data. Since the 2MASS positions are highly accurate, and both the 2MASS images and DSS images are (or will shortly be) easily accessible electronically, we are not presenting finding charts.

Using the available parallaxes for late-type dwarfs (Monet et al. 1992; Tinney et al. 1995; Tinney 1996; Kirkpatrick et al. 1999b), we find (Fig. 1) the linear fit $M_K = 7.593 + 2.25 \times J-K_s$ This fit is valid only for M7 and later dwarfs over the color range $1.0 \leq J-K_s \lesssim 1.6$ and should be modified as more L dwarf parallaxes are measured at USNO. The observed scatter is $\sigma = 0.36$ mag. The distances and tangential velocities derived using this estimate are listed in Table 3. We caution, however, that the distances derived for many of the M7 and M7.5 dwarfs may be underestimated in this paper. As can be seen in Figure 1, the main sequence bends sharply at spectral type M7. Our selection of only targets with $J-K_s \geq 1.0$ tends to select M6's and M7's with overestimated colors, while a spectral classification error of only 0.5 subclasses from M6.5 to M7.0 leads to a large error in M_K.

3. STARS OF SPECIAL INTEREST

A few of the targets deserve special comment. Our search has identified one very nearby star and a number of very high proper-motion dwarfs. The M8.0 dwarf 2MASSW J0027559+221932 has a photometric parallax that places it within 10 pc; given the uncertainties, it may lie within the 8 pc sample. We note also that a number of dwarfs in Table 3 have motions greater than $1'' \text{ yr}^{-1}$ but do not appear in the LHS Catalog even though they are visible on the POSS plates.

Seven L dwarfs are part of our Sample BC. The L5 dwarf 2MASSW J1507476−162738, also in Reid et al. (2000), was selected for this project but does not lie in the Sample BC area. Additional observations and discussion of 2MASSI J0746425+200032, 2MASSW J0036159+182110, and 2MASSW J1439283+192915 are given in Reid et al. (2000). 2MASSW J1439283+192915 is in the original K99 paper, while 2MASSW J0036159+182110 was observed at Keck for the K00 paper. 2MASSW J1300425+191235 is particularly surprising: it has the $J-K_s$ color of an M8 dwarf but has an L1 spectrum. It will be discussed further in an additional paper, but we note here that the estimated distance and tangential velocity is based on the $J-K_s$ color and should be viewed with great caution. Nevertheless, it apparently has a high velocity and is likely to be old. While we report photometric distance estimates only, most of these dwarfs are on the USNO parallax program, and accurate distances should be forthcoming.

Since our selection is based upon photometry only, we are sensitive to wide binary pairs in which the 2MASS observations of the secondaries are unaffected by the primaries. Two M dwarf secondaries that do not meet the spatial restrictions and were specially observed have been reported in Gizis et al. (2000). One of the Sample C ultracool M dwarfs also appears to be a secondary. The M8.0 dwarf 2MASSW J2331016−040618 is 447″ west and 65″ south of the F8 dwarf HD 221356. Our photometric parallax of 26.3 pc for the M dwarf is consistent with *Hipparcos* trigonometric parallax of 26.24 pc (Perryman et al. 1997), as are the observed proper motions. This is apparently a wide binary system with separation of 0.057 pc. The F8 primary may provide a useful age and composition constraint on the M dwarf.

Two of our sources have been previously identified as candidate Hyades members. LP 475-855 has been discussed as an Hyades candidate by Eggen (1993), although it was rejected as too bright by Leggett, Harris, & Dahn (1994). Our photometry supports the latter conclusion, although conceivably it could be a foreground (escaping?) Hyades member if it is an unresolved equal-mass binary. Our initial observation of this star found it in a flare state, with Hα equivalent width of 40 Å. A 1998 December 25 Keck spectrum found Hα of only 7 Å, which is the value we report in Table 1. LP 415-20 (Bryja 262) has been extensively discussed as a Hyades member and has been classified as an M6.5 dwarf (Bryja, Humphreys, & Jones 1994). The difference in spectral types is within our uncertainties, and we note that VO is visible in Bryja's plot of the spectrum. The

poor distance estimate for this object is consistent with our belief that our M7 distances based on $J-K_s$ colors are unreliable and should be viewed with caution.

4. COLORS

In Figure 2, we plot the $R-K_s$, $J-K_s$ diagram for Sample B. We concluded that adjusting our color criterion to $R_F-K_s>4.9$ would increase our selection efficiency without losing M8 and later dwarfs, and we adopted this selection criterion for Sample C. This observation is consistent with our estimate that our simple R_F zero point is good to ± 0.5 mag.

Our observations show a good correlation between the far-red spectral type and the 2MASS near-IR colors. In Figure 3, we plot the observed $J-K_s$ color distribution as a function of spectral type. As expected, the M7.0 and M7.5 distributions are truncated by our requirement that $J-K_s \geq 1.0$. The histograms suggest that of order one M8–M8.5 dwarf may be expected to be missed owing to this requirement, and it appears that it is very unlikely than any (normal) M9 dwarfs are missed. 2MASS photometry for these bright sources is expected to be good to 0.03 magnitudes.

In Figure 4, we plot the 2MASS near-infrared color-color diagram for our sample. It is evident that the M/L dwarf sequence lies well below our imposed $J-H$, $H-K$ cut, and therefore we are not missing ultracool M dwarfs due to this criteria. We fit the relation $J-K_s=(0.146\pm0.117)+(1.238\pm0.263)\times H-K_s$ assuming the errors in each color are 0.042 and including the M7.0–M9.5 dwarfs. This relation may be convenient as a representative sequence in the 2MASS color system. It is interesting to note that the dwarfs around $(H-K,\ J-H)=(0.45,\ 0.62)$ are nearly all

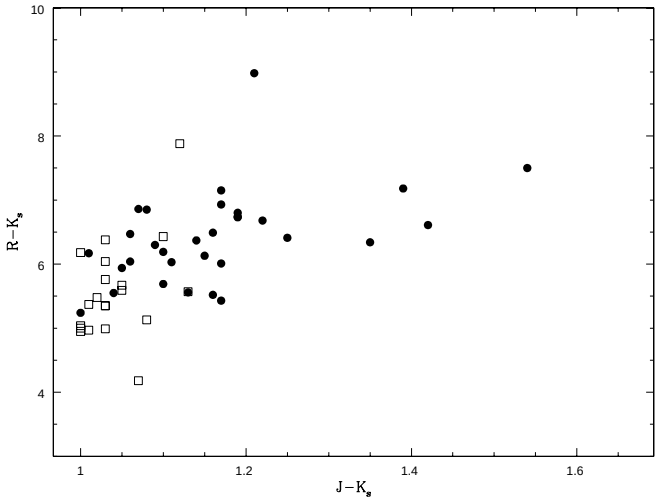

FIG. 2.—Color-color diagram for the December sample using the photographic R and 2MASS J and K_s magnitudes. M8 and later dwarfs are filled circles, M7 dwarfs are filled squares, and M6 and earlier dwarfs are crosses. A selection on $R-K_s>4.9$ would improve our efficiency without excluding the ultracool M dwarfs.

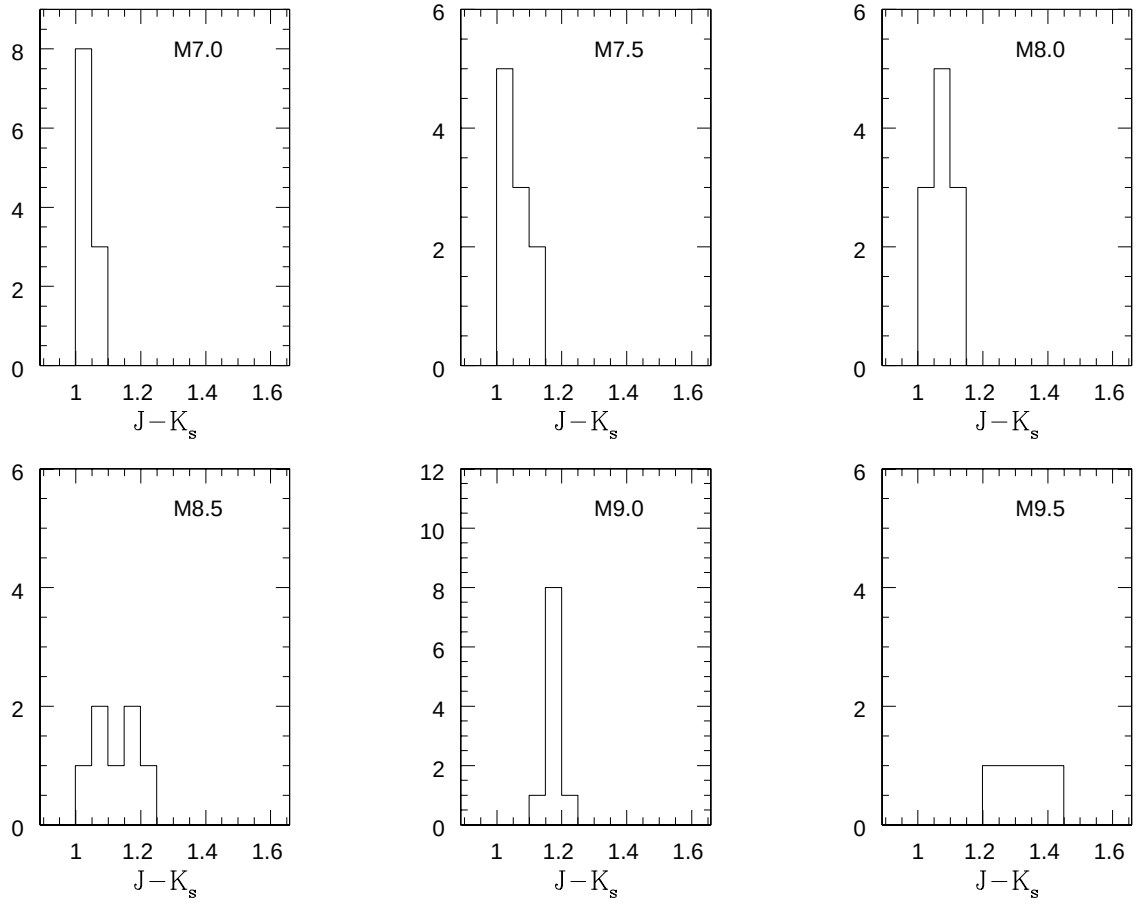

FIG. 3.—2MASS $J-K_s$ color as a function of spectral type. Each bin is 0.05 magnitudes wide, approximately equal to the 2MASS uncertainty. Note the correlation between infrared color and far-red spectral type.

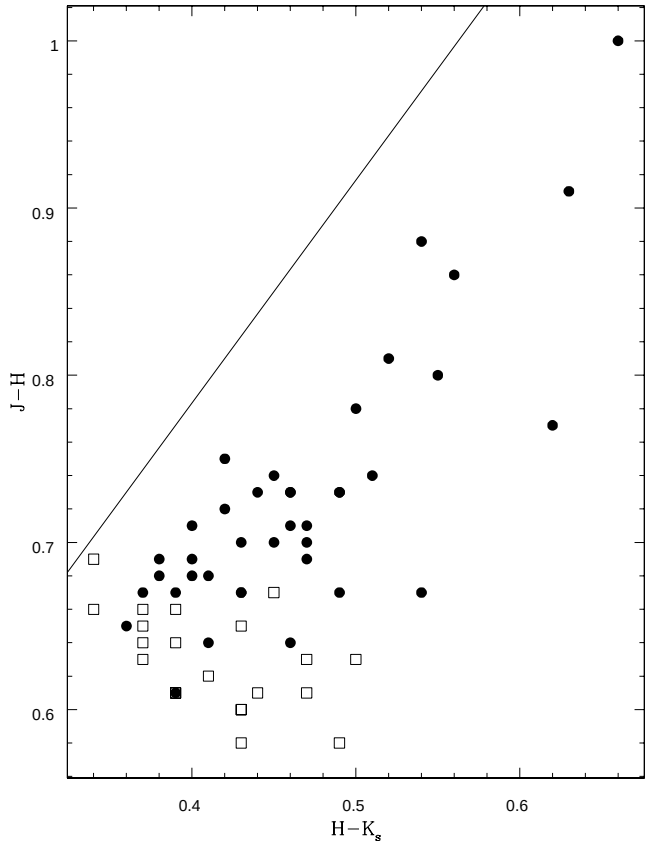

FIG. 4.—2MASS near-infrared color-color diagram. The solid lines indicate our selection criterion. Note that all the M and L dwarfs lie well below the line intended to exclude giants.

classified as M7–M7.5 dwarfs, while the dwarfs at $(H-K, J-H) = (0.42, 0.7)$ but with similar $J-K_s$ colors are nearly all classified as M8–M8.5 dwarfs. This may reflect some relation between the red–optical region (dominated by TiO and VO, and influenced by dust) and the IR colors (dominated by H_2O and H_2, and also influenced by dust)—or it is due to some subtle bias in our classifications or photometry (for example, perhaps we tend to select M7 dwarfs whose $H-K_s$ color has been overestimated). Note that one of the outliers below the normal $J-H$, $H-K_s$ relation is the peculiar L dwarf 2MASSW J1300425+191235.

5. LUMINOSITY FUNCTION

Our Sample BC is the first large sample of bright, photometrically selected ultracool M dwarfs. Using our data and derived distances, we can estimate the luminosity function using Schmidt's (1968) $V/V_{\max}$ technique. The space density is

$$\Phi = \sum \frac{1}{V_{\max}}$$

$$V_{\max} = \frac{\Omega}{3}\left(10.0^{(K_{\lim} - M_K + 5.0)/5.0}\right)^3 .$$

In our case, $K_{\lim} = 12.0$ and $\Omega = 6040$ deg^2. The corresponding variance is

$$\sigma_\Phi^2 = \sum \frac{1}{V_{\max}^2} .$$

The space densities are given in Table 4. We derive a space density of 0.0045 ± 0.0008 ultracool M dwarfs per cubic parsec. According to our adopted color-magnitude relation, this is for dwarfs in the range $9.8 < M_K < 10.8$. Therefore, the corresponding luminosity function bin is $\Phi(M_K = 10.3) = 0.0048 \pm 0.0009$ dwarfs per cubic parsec per K magnitude. Since Tinney et al. (1993) have shown that $BC_K = 3.2$ for these late dwarfs, this may be represented in bolometric magnitudes as $\Phi(M_{\rm bol} = 13.5) = 0.0048 \pm 0.0009$ dwarfs per cubic parsec per bolometric magnitude. We note, however, that this value excludes the M7 dwarfs which will also contribute near $M_K = 9.8$, so our value is a lower limit. The space density for the early L dwarfs is half that of the ultracool M dwarfs, although we caution that the distance estimate for 2MASSW 1300425+191235 may be incorrect.

Schmidt's statistic measures the uniformity of the density distribution of a sample, effectively providing an estimate of sample completeness. For a uniform sample, $\langle V/V_{\max}\rangle = 0.5$ with an uncertainty of $1/(12N)^{1/2}$, where N is the number of stars observed. Both our L dwarf and M8.0–M8.5 sample lie within 1 σ of this value, suggesting that we are complete. The value for M9.0–M9.5 dwarfs is more problematic, indicating that we have either excluded a few nearby, very bright M9 dwarfs, or that there happen to be no such very nearby dwarfs in our survey volume.

Our space density for the ultracool M dwarfs is consistent with Tinney's (1993) value of $\Phi(M_{\rm bol} = 13.5) = 0.0076 \pm 0.0031$ dwarfs per cubic parsec per bolometric magnitude, which was based on selection with R_F and I_N photographic magnitudes but K follow-up of all VLM dwarfs to improve photometric parallaxes. Only six dwarfs contributed to this bin, accounting for Tinney's larger uncertainty relative to our sample. Delfosse et al. (1999) have analyzed the DENIS Mini-survey and found 19 M8 and later dwarfs, including three L dwarfs. They do not estimate the M dwarf space density but use the three L dwarfs to estimate $\Phi(M_{\rm bol} = 15.3) \geq 0.011 \pm 0.006$ dwarfs per cubic

TABLE 4

SPACE DENSITIES

Sp. Type	N	Φ	σ_Φ	Units	$\left\langle \frac{V}{V_{\max}} \right\rangle$	$\sigma_{\langle V/V_{\max}\rangle}$
M8.0–M8.5.....	17.	1.90	0.47	10^{-3} stars pc^{-3}	0.56	0.07
M9.0–M9.5.....	15.	2.57	0.69	10^{-3} stars pc^{-3}	0.71	0.07
M8.0–M9.5.....	32.	4.46	0.83	10^{-3} stars pc^{-3}	0.63	0.05
L0.0–L4.5	7.	2.11	0.92	10^{-3} stars pc^{-3}	0.53	0.11
M8.0–L4.5	39.	6.57	1.24	10^{-3} stars pc^{-3}	0.61	0.05
M8.0–M9.5.....	32.	4.75	0.89	10^{-3} stars pc^{-3} mag^{-1}	0.63	0.05
M8.0–L4.5	39.	4.38	0.83	10^{-3} stars pc^{-3} mag^{-1}	0.61	0.05

parsec per bolometric magnitude. We note that their estimated M_K for the ultracool M dwarfs are inconsistent with our adopted values (and Fig. 1) since they consider their M8–M9 dwarfs to have $M_K > 11$.

Malmquist bias will affect our sample. Stobie, Ishida, & Peacock (1989) have shown that the luminosity function will be overestimated by

$$\frac{\Delta\Phi}{\Phi} = 0.5\sigma^2\left[(0.6\ln 10)^2 - 1.2\ln 10\,\frac{\Phi'}{\Phi} + \frac{\Phi'}{\Phi''}\right].$$

A model luminosity function can be used to derive the first and second derivatives. The scatter of parallax stars about the linear fit adopted here is $\sigma = 0.36$. Adopting this value for σ, and making the assumption that the luminosity function is flat, we find that $\Delta\Phi/\Phi = 0.21$: i.e., the values we derive overestimate the true space densities by $\sim 20\%$. Since this is only a preliminary sample, we defer further analysis of the Malquist bias, as well as the effect of unresolved binaries, until additional data are available. In the long term, trigonometric parallaxes and searches for companions will allow this issue to be addressed directly.

Our derived space density can best be compared to the luminosity function of nearby stars. Figure 5 plots the Reid & Gizis (1997) ($\delta > -30°$) luminosity function for stars within 8 pc with our M8.0–L4.5 data point added to it. Our results suggest that the drop-off seen in for the faintest ($M_K > 10$) dwarfs in the 8 pc sample is in part due to incompleteness.[4] Applying standard mass-luminosity relations to $\Phi(M_K)$ derived from the 8 pc sample implies a turnover in the mass function close to the hydrogen-burning limit. There is, however, no reason to expect the star formation process to be cognizant of the mass limit for hydrogen burning. Reid et al. (1999b) have modeled a sample of 20 2MASS and three DENIS L dwarfs and conclude that the substellar mass function is consistent with an extension of the power law matched to data for stars with masses between 0.1 and 1 $M_\odot$. The higher space densities measured for ultracool dwarfs in this paper suggest a greater degree of continuity across the stellar/substellar boundary. Continuation of the present survey should identify the missing dwarfs within 8 pc.

If compared to the classical "photometric" luminosity functions (Stobie et al. 1989; Tinney 1993), which have a peak at $M_{\rm bol} = 10$ and a drop-off to $M_{\rm bol} = 12$, then our data would imply a rise in the luminosity function at the stellar/substellar boundary. However, this peak and drop-off are an artifact of the data analysis due to the incorrect assumption of a linear color-magnitude relation (Reid & Gizis 1997) and/or other systematic errors such as unresolved binaries (Kroupa, Tout, & Gilmore 1993). We believe that the nearby star sample is a better comparison for our sample, and we emphasize again that the M dwarfs here identified require follow-up trigonometric parallax determinations and high-resolution imaging and radial velocity searches for companions to produce a definitive luminosity function.

6. ACTIVITY AND KINEMATICS

6.1. *Review*

The BC sample was not selected on the basis of proper motions and therefore is (relatively) unbiased in terms of kinematics.[5] It is useful to review the properties of nearby disk stars and the already known properties of ultracool M dwarfs before discussing our kinematic and activity measurements.

Stars are born with low space velocity dispersions and high chromospheric activity levels. Over time, the space velocity of the stars increases as they interact with the Galactic disk. Using BAFGK dwarfs with known ages, Wielen (1974) showed that the total space velocity increases from $\sigma_{\rm tot} = 19$ km s^{-1} at mean ages of 0.4 to 0.9 $\times$ 10^9 yr to 34 km s^{-1} at 2 $\times$ 10^9 yr to 48 km s^{-1} at 5 $\times$ 10^9 yr. The high chromospheric activity levels of young stars with convective envelopes are attributed to a dynamo that is driven by rotation. As the star ages, angular momentum loss through the stellar wind spins down the star, causing the chromospheric activity to in turn decrease. Wielen (1974) did indeed find that Ca II emission-line strength in M dwarfs was related to kinematics, with older stars showing less activity and higher space velocities. As progressively less massive (later spectral type) stars are considered, the observed frequency of high Hα activity increases. This is *not* due only to the fact that Hα emission is more detectable against the cool photosphere—Hawley, Gizis, & Reid (1996, hereafter HGR) showed that the percentage of highly active M dwarfs increases with cooler spectral types even when Hα activity is compared to the star's bolometric luminosity. The increased lifetime of activity is confirmed by observations of open clusters Hawley, Reid, & Tourtellot (1999b). The connection to rotation in early M dwarfs is confirmed by Delfosse et al. (1998), who have found that the incidence of rapid rotators is higher among cooler M dwarfs and that

[4] Note that, as seen in Reid & Gizis's Fig. 2, the oft-used 5.2 pc sample shows the same feature, albeit with less significance owing to the very small volume.

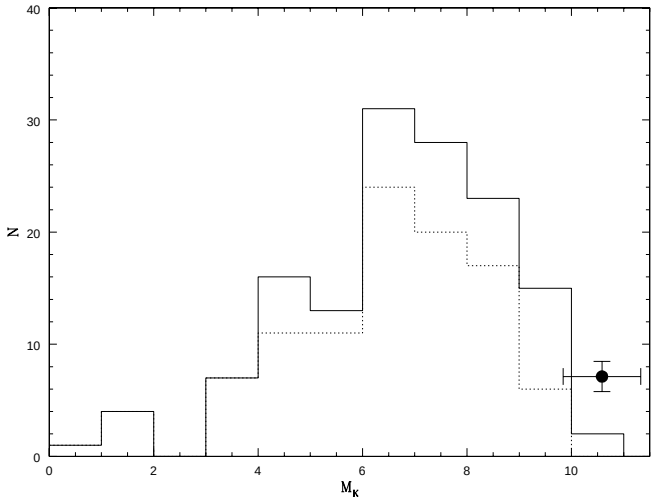

FIG. 5.—Our observed space density of cool (M8.0–L4.5) dwarfs compared to the Reid & Gizis (1997) 8 pc sample (as updated in Reid et al. 1999b). The solid histogram count known secondaries, while the dotted histogram excludes them. The steep dropoff at $M_K > 10.0$ seen in both the 8 and 5.2 pc samples is moderated by our space density.

[5] The existence of age-luminosity, age-metallicity, metallicity-luminosity, age-activity, and age-kinematics correlations implies that there may be kinematic and/or activity bias due to our Malquist-type luminosity bias. If the distances are underestimated owing to bias, then the estimated tangential velocities will also be biased.

the rapid rotators are active. There is some evidence that the rotation-activity relation is breaking down (Hawley, Reid, & Gizis 1999a). In summary, mid-M dwarfs maintain Hα emission for billions of years as they slowly spin down. Kinematics are a good age indicator, but only in a statistical sense—individual stars can not be accurately dated by the velocities.

For the ultracool M dwarfs, there is considerable evidence that the standard stellar age-activity and rotation-activity relations no longer apply. Basri & Marcy (1995) found that the M9.5 dwarf BRI 0021−0214 had very rapid rotation ($v \sin i = 40$ km s^{-1}) but little Hα activity. TR have shown that the lithium M9 brown dwarf LP 944-20 (Tinney 1998) is also a member of this class of "inactive, rapid rotators" as are the two of the DENIS L dwarfs (Martín et al. 1997). TR argue that observations of these field objects as well as open clusters indicate that the violation of the age-activity connection is primarily correlated with mass (the physical mechanisms remain unknown). Basri (1999) reports that rapid rotation is more common among objects of lower luminosity and proposes that the Hα activity is powered by a turbulent dynamo that is quenched at high rotation rates. There is some evidence that even among the "inactive, rapid rotators" $\log (L_{H\alpha}/L_{bol})$ is related to age, as it decreases from ~ -4.6 for the Pleiades to ~ -5.2 for ~ 0.5–1.0×10^9 yr brown dwarfs. This trend may be true for younger ages, since the very low mass (~ 0.01–$0.06\ M_\odot$), very young (<10 Myr) M8.5 brown dwarf ρ Oph 162349.8−242601 has $EW_{H\alpha} > 50$ Å (Luhman, Liebert, & Rieke 1997; Martín, Basri, & Zapatero-Osorio 1999a), while the young (~1 Myr), possible brown dwarfs ($M \approx 0.07\ M_\odot$) V410 Tau X3 (M8.5) and X6 (M6) have $EW_{H\alpha} \approx 15$ Å (Martín et al. 1999a). Both imply higher activity levels than their older Pleiades and field counterparts, though it should be noted that they are also lower mass. In contrast to the "inactive, rapid rotators," some ultracool M dwarfs do show Hα emission, but they have lower rotation rates ($\lesssim 20$ km s^{-1}; TR). However, even a rotation rate of ~5 km s^{-1} is adequate to maintain Hα emission in mid-M dwarfs (Bopp & Fekel 1977), so the limits on the "low" rotation rates of these ultracool M dwarfs are not surprising by comparison. A so-far unique field object is the M9.5 dwarf PC 0025+0447 (Schneider et al. 1991; Martín et al. 1999a), whose quiescent Hα emission (300 Å) is comparable to highly active mid-M dwarfs in terms of $L_{H\alpha}/L_{bol}$. The nature of this object and its emission is uncertain—Martín et al. (1999a) argue that this object is a very young brown dwarf, suggesting that the USNO parallax indicating ordinary ultracool M dwarf luminosity is incorrect. Some of the known M8–M9 dwarfs are definitely brown dwarfs. The "inactive, rapid rotator" M9 dwarf LP 944-20 has lithium absorption and a luminosity that indicates it has a mass between 0.056 and 0.064 $M_\odot$ (Tinney 1998). The Pleiades brown dwarfs Teide 1 and Calar 3 have spectral types of M8, lithium absorption, and anomalous VO and Na features due to low surface gravity (Martín, Rebolo, & Zapatero-Osorio 1996).

6.2. *The Properties of M and L Dwarfs*

The BC sample of ultracool M dwarfs provides the first opportunity for a thorough investigation of the distribution of activity in these VLM dwarfs. In Figure 6, we compare the percentage of ultracool M dwarfs observed in emission to the HGR statistics for nearby K7–M6.5 dwarfs. Note

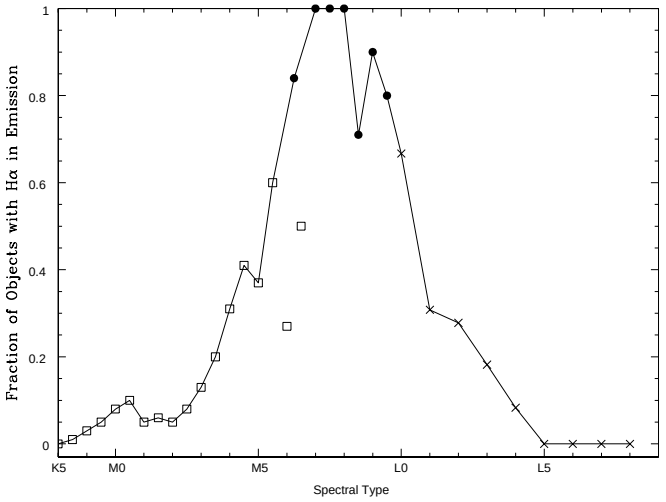

FIG. 6.—Observed percentage of Hα emission line dwarfs among K5–M6.5 dwarfs (HGR; *open squares*), M6–M9.5 dwarfs (this paper; *filled circles*), and L0–L8 dwarfs (K99, K00; *crosses*). K5 and K7 dwarfs are plotted as −2 and −1, respectively, while the L dwarfs are plotted with 10 added to their subclass. The HGR M6 and M6.5 dwarfs may be affected by kinematic bias, leading to an underestimate of the number of emission stars. The solid line connects the three studies, adopting this paper's values for M6 dwarfs over the HGR values.

that ~80 to ~300 dwarfs contribute to each of the HGR bins up to spectral type M4.5. Only a few objects contribute to the M6.0 and M6.5 bins, which also are probably kinematically biased against young, active stars owing to incompleteness in the pCNS3.[6] We extend our M dwarf sample to even cooler dwarfs by using the K99 and K00 data, who report the strength of Hα emission in their L dwarfs. Their sample is photometrically selected and kinematically unbiased. The sample shows a steady decline in Hα emission frequency from 60% (80% if a marginal detection is included) for type L0 down to only 8% (25% if two marginal detections are included) for L4 dwarfs. None of the 20 dwarfs with spectral type L5.0 or later show definite emission (two have marginal detections). For the earlier dwarfs, emission of 1 Å equivalent width would have been detected in almost all the objects; however, the upper limit on the equivalent widths for the latest L dwarfs was typically somewhat larger. The fact that there is so little photospheric continuum for the latest L dwarfs around the Hα feature should compensate for the lower sensitivity in terms in equivalent widths.

The data indicate that the frequency of emission increases with later spectral type (cooler temperatures) until at spectral type M7 all of our targets show detectable emission. Indeed, we are not aware of *any* inactive M7 dwarfs (HGR; Gizis & Reid 1997). This indicates that the dwarfs can maintain detectable levels of activity for the lifetime of the Galactic disk. Later than M7, the Hα emission frequency begins to decrease, with our sample of ultracool M dwarfs merging cleanly with the L dwarfs. This coincides with the breakdown of the rotation-activity relation already noted for M9 and L dwarfs and reflects the apparent relative inability of the ultracool M dwarfs to heat the chromosphere discussed

[6] HGR's statistics for M7 and later dwarfs are sparse, but further observations have revealed that they are incorrect. Their Table 5 should show that two of two M7 dwarfs, two of two M8 dwarfs, and two of three M9.0–M9.5 dwarfs show emission.

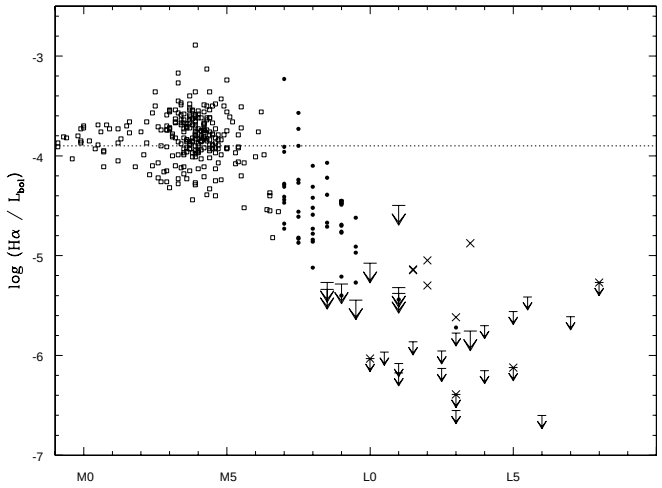

FIG. 7.—Hα luminosity relative to the bolometric luminosity as a function of spectral type for our ultracool M dwarfs (*filled circles*), the earlier M dwarfs of HGR (*open squares*), and the L dwarfs of K99 (*crosses*). For our ultracool M dwarfs, approximate upper limits are plotted assuming an Hα equivalent width of 2 Å. The dotted line at −3.9 is the level at which any M dwarf would be observed in emission. None of the M8 or later dwarfs have activity levels above the −3.9 level.

by TR. The percentage of emission at spectral type M6 is particularly uncertain, as the HGR sample may be biased toward higher velocity, hence older, stars at such low luminosities. Sixteen of our 19 M6–M6.5 dwarfs show emission, but they have been effectively selected on the basis of unusually red $J-K_s$ colors and may be biased in some way. In any case, there is little doubt that some high-velocity, presumably very old, M6 dwarfs are no longer active.

Since the Hα line is seen against an increasingly faint photosphere for these ultracool dwarfs, the log $(L_{H\alpha}/L_{bol})$ ratio is more indicative of the true level of activity. We plot our M dwarfs, the HGR early M dwarfs, and the K99 L dwarf data in Figure 7. For the K99 data, we have measured the continuum level off the observed spectra and assumed $BC_K = 3.33$ as measured by Tinney et al. (1993) for GD 165B to convert the K99 equivalent widths to flux ratios. Note that the increase in maximum observed activity levels from K7 to the peak at M3–M5 reflects the increased lifetime of emission for the lower mass stars. Earlier M dwarfs with activity levels near −3 are known in young clusters but do not have long enough lifetimes to appear in the local sample. The lower envelope of data points is set by the fact that the minimum observable Hα emission of 1 Å equivalent width corresponds to a lower luminosity fraction in cooler dwarfs. The addition of our data to the HGR data clearly indicates that beyond M7 the level of activity is indeed declining. This decline continues for lower (L dwarf) temperatures. The decline is quite steep—in only three subclasses (M8–L1) the activity drops by one full dex. Martín et al. (1999b) note a "slight trend toward decreasing emission in the L dwarfs"—our conclusions differ owing to our larger sample and their use of equivalent widths only.

While the quiescent Hα chromospheric activity is declining, our data suggest that flare activity is common in the ultracool M dwarfs and may be a significant contributor to the activity energy budget. We summarize evidence for variability in Table 5. Since these events represent a strong enhancement of the Hα line strength, we suggest that they may be flares. At least a few dwarfs apparently maintain strong quiescent emission—our Hα line strength of 29 Å for LP 412-31 is identical with the value observed by Martín et al. (1996). Other ultracool M dwarfs not in our sample have been seen to flare—Reid et al. (1999a) recently observed a flare on the "inactive" dwarf BRI 0021−0214, while Martín, Rebolo, & Magazzu (1994) observed the Hα EW of LHS 2065 on two consecutive nights as 7.5 Å and then 20.3 Å. Martín et al. (1999b) have observed flares in a number of ultracool M dwarfs. Flaring activity has thus been observed in ultracool M dwarfs with both very low and high levels of quiescent emission.

Assuming that these strong variations are due to flares, we estimate the flare rate from our own statistics. At least four of the 53 ultracool M targets were flaring the first time we observed them for this program—implying that ultracool M dwarfs spend $\gtrsim 7\%$ of the time in a flare state. This is consistent with the observed flare rates of the "inactive" M9.5 dwarf BRI 0021−0214 (Reid et al. 1999a) and the monitoring of 2MASSI J0149089+295613 (Liebert et al. 1999). This flare rate is a lower limit, since some of our other targets may also be flaring, but lacking additional spectra we cannot tell whether they are merely active as for LP 412-31, and since we have no way of identifying weaker flares. The Hα equivalent widths appear to be enhanced by a factor of ∼10 in the observed flares, implying that perhaps half of the Hα luminosity is emitted during flares.

We now consider the relationship between kinematics and activity for the M8–M9.5 dwarfs. In Figure 8, we plot the observed relation between the tangential velocity and Hα emission. There is a striking relationship between activity and velocity, in a sense opposite to that observed in more massive M dwarfs. All the dwarfs with strong Hα emission have large velocities ($v_{tan} > 20$ km s^{-1}). There is also a striking population of low-velocity, low-activity ultracool M dwarfs. With the exception of the high-velocity, inactive M9 dwarf 2MASSW J0109216+294925, the least active stars appear to be drawn from a lower velocity popu-

TABLE 5

FLARES

Name	Sp.	Hα	Source	Flare Hα	Source
2MASSW J0149089+295613.....	M9.5	11.0	L99	300	L99
2MASSW J2234138+235956.....	M9.5	4.4	KPNO	20	Keck
LHS 2397a	M8	15	LCO	?	B91
LHS 2243	M8	1.3	M94	44	LCO
LP 475-855	M7	7	Keck	40.5	LCO

NOTE.—Sources are LCO (Las Campanas, this paper), KPNO (Kitt Peak, this paper), Keck (Keck, this paper), B91 (Bessell 1991), M94 (Martin, Rebolo, & Maguzzu 1994), L99 (Liebert et al. 1999).

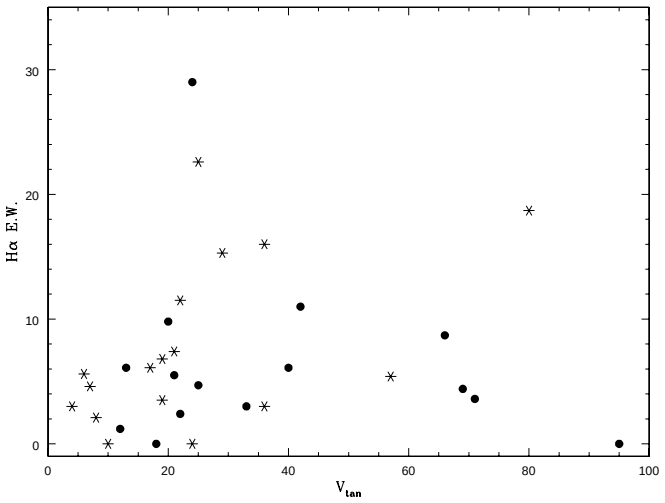

FIG. 8.—Hα equivalent width as a function of tangential velocity. M8.0–M8.5 dwarfs are plotted as stars, and M9.0–M9.5 dwarfs are plotted as filled circles. All M8–M9 dwarfs with Hα equivalent widths over 10 Å have large space velocities. Note 2MASSW J0109216+294925, which has no emission but a high tangential velocity.

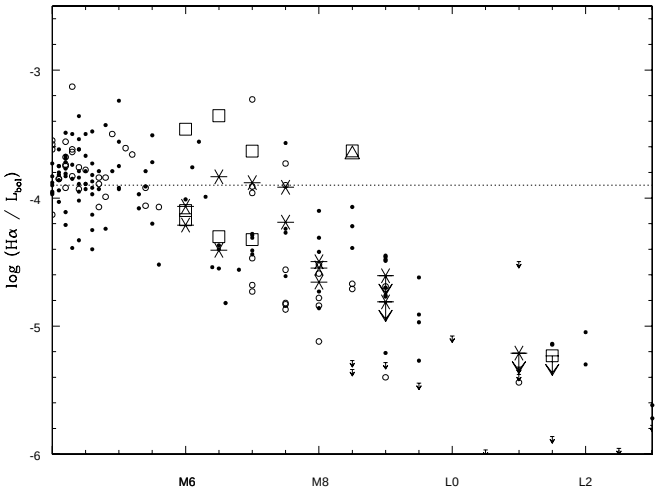

FIG. 9.—Hα luminosity relative to the bolometric luminosity as a function of spectral type for both cluster brown dwarfs and field dwarfs. Brown dwarfs from the σ Ori cluster ($<10^7$ yr), ρ Oph ($<10^7$ yr), Pleiades ($\sim 10^8$ yr) are shown as open squares, open triangles, and six-pointed stars, respectively. Note that both cluster L dwarfs have only upper limits on the detected Hα emission. The field M dwarfs are plotted as open circles if $v_{\rm tan} < 20$ km s^{-1} and filled circles for higher velocities.

lation. It is difficult to fairly characterize the tangential velocity dispersion $[\sigma_{\rm tan}^2 = (\sigma_{\rm ra}^2 + \sigma_{\rm dec}^2)^{1/2}]$ of these populations, but the inactive, low-velocity population in the lower left of Figure 8 may be characterized by $\sigma_{\rm tan} \approx 15$ km s^{-1}. While the low-velocity, low-activity population seems to have $EW_{H\alpha} \lesssim 7$ Å and $v_{\rm tan} \lesssim 25$ km s^{-1}, we can calculate a velocity dispersion only for a purely activity selected sample. As an illustration, the dwarfs with $EW_{H\alpha} < 3$ Å (excluding 2MASSW J0109216+294925) have $\sigma_{\rm tan} = 13$ km s^{-1}; in contrast, those with more emission have $\sigma_{\rm tan} = 38$ km s^{-1}. Using the approximation that $\sigma_{\rm tot} = (3/2)^{1/2}\sigma_{\rm tan}$, the implied total space dispersions of the two populations are 16 and 47 km s^{-1}. Comparing to Wielen (1974), the active M dwarfs are apparently drawn from a $\sim 5 \times 10^9$ yr population, but the inactive M dwarfs are consistent with a ~ 0.5 Gyr population. This estimate is crude at best, but it seems clear that the overall ultracool M dwarf population is drawn from a long-lived, presumably stellar population, while the group of less active, low-velocity stars represent a younger ($\lesssim 1$ Gyr) population .

Despite the smaller sample size, the properties of L dwarfs are of considerable interest. The Sample BC L0–L4 dwarf velocities are typical of an old disk population. Even excluding 2MASSW 1300425+191235 owing to unusual color, we find $\sigma_{\rm tan} = 56$ km s^{-1}, while including it we find $\sigma_{\rm tan} = 70$ km s^{-1}. Only two of the Sample BC L dwarfs show emission—the low-velocity 2MASSW J1108307+683017 has the strongest emission at 7.8 Å, while the high-velocity 2MASSW 15066544+132100 has weak 1 Å emission. While the velocities of only two L dwarfs are not definitive, the velocity distribution of the inactive L dwarfs suggest they are mostly old. Adding the information provided by the work of K99 and K00 to our data provides strong clues that, just as in the ultracool M dwarfs, the traditional activity-age relationship is broken, perhaps even reversed. L dwarfs that show lithium absorption are necessarily younger and lower mass than L dwarfs of the same spectral type that have destroyed lithium. Thus, using the traditional stellar age-activity relation, one would expect them to be more chromospherically active. Consider the L1–L4.5 dwarfs, where lithium is detectable even at the low resolution of the K99/K00 Keck LRIS observations. Only one L dwarf, Kelu 1, shows both Hα emission and lithium absorption.[7] Eleven other such L dwarfs show Hα emission but do not have lithium absorption. Twelve L dwarfs show lithium absorption but do not have Hα emission (four of these have marginal Hα detections or noise consistent with emission of less than 2 Å). While many L1–L4 dwarfs have neither Hα emission nor lithium absorption, it seems clear that the chromospherically active L dwarfs are drawn from an older, more massive population than the lithium L dwarfs. Beyond L4.5, there are no definite cases of Hα emission, although lithium absorption is present for $\sim 50\%$ of the L dwarfs.

Brown dwarfs have also been identified in nearby young clusters. In Figure 9, we compare the activity of our field dwarfs to young brown dwarfs. Shown are young brown dwarfs from the σ Ori cluster (Bejar, Zapatero-Osorio, & Rebolo 1999; Zapatero-Osorio et al. 1999) and the young brown dwarf in the ρ Oph cloud (Luhman et al. 1997)—both these clusters are less than 10 Myr old. Also shown are confirmed Pleiades brown dwarfs (Martín et al. 1996; Zapatero-Osorio et al. 1997; Martín et al. 1998a; Martín et al. 1998b) with age $\sim 10^8$ yr. In order to suggest the age evolution of the field M dwarfs, those with $v_{\rm tan} < 20$ km s^{-1} have been shown as open symbols. These low-velocity dwarfs are likely to be younger than the other field dwarfs. It is evident that the Pleiades M8 and later brown dwarfs are not more active that the typical field dwarfs, although the M6–M7 brown dwarfs appear to be more active. Like the young field L dwarfs that have lithium absorption, the Pleiades and σ Ori L dwarfs do not show emission, even though some older field L dwarfs do. In the case of the ρ Oph brown dwarf, Luhman et al. (1997) have shown that the emission is probably due to accretion from the circumstellar disk or envelope detected in the mid-IR. Similar acc-

[7] It is interesting to note that Basri (1999) finds that Kelu 1 is rotating extremely rapidly: 80 km s^{-1}.

retion may account for the σ Ori strong emitters, while the absence of accretion would account for the weak emission in the other half of the σ Ori brown dwarf sample. If the emission is chromospheric, then some other factor (such as rotation) is needed to explain the large spread in activity levels. It should be noted that these young brown dwarfs are probably hotter at a given spectral type (Luhman, Liebert, & Rieke 1997), which suggests that if temperature were plotted, the brown dwarfs would appear even less active compared to field dwarfs.

We thus summarize the observations:

1. Although the fraction of dwarfs showing Hα emission reaches 100% at spectral type M7, the fraction that shows chromospheric activity drops rapidly for later spectral types.
2. The fraction of energy in chromospheric Hα for those dwarfs that are active drops rapidly as a function of spectral type beyond M6.
3. Low-velocity, kinematically young M8.0–M9.5 dwarfs have weaker activity than many higher velocity, old M8.0–M9.5 dwarfs.
4. Flaring is common among the M7–M9.5 dwarfs.
5. The early L (L0–L4) dwarfs in Sample BC have old kinematics.
6. Early L (L1–L4.5) dwarfs with Hα emission are old and massive enough to have burned lithium.
7. L1–L4.5 dwarfs with lithium are unlikely to have Hα emission.
8. None of the L dwarfs later than L4.5 have Hα emission, but half have lithium.
9. The two known L dwarfs in young clusters do not show Hα emission
10. Young Pleiades M8–M9 dwarfs are less active than the higher velocity field M dwarfs.

6.3. *Discussion*

How can these observations be explained? We believe they imply that the maximum activity level is a strong function of temperature beyond spectral type M7, with lower temperature objects able to maintain less emission. Additionally, beyond spectral type M7 substellar dwarfs tend to have less activity than stellar dwarfs.

In Figure 10, we plot evolutionary sequences from Burrows et al. (1993) and Baraffe et al. (1998). In the Baraffe et al. (1998) models the hydrogen-burning limit is at 0.072 $M_\odot$, and the lithium-burning limit is at 0.055 $M_\odot$. Also shown is an estimated temperature scale from Reid et al. (1999b) based on the arguments made in K99. The models indicate that it takes $\gtrsim 10^9$ yr for stars near the hydrogen-burning limit to settle into the M8 and cooler temperatures (Fig. 10). M8 and cooler temperatures are possible at younger ages, but they are substellar objects that continue to cool with time. Thus, the low-velocity, low-activity population is likely to be a population of substellar/transition objects. By the time they are older than 1 Gyr, they appear as L dwarfs or even cooler T dwarfs. Thus, the comparison of low-velocity M8–M9.5 dwarfs to high-velocity M8–M9.5 dwarfs is the same as a comparison of younger, lower mass ($\sim$0.07 $M_\odot$) objects to older, higher mass objects ($\sim$0.08 $M_\odot$) at the same temperature. The same occurs when comparing the K99/K00 lithium L1–L4 ($\sim$0.055 $M_\odot$) dwarfs to the K99/K00 non-lithium L1–L4 ($\sim$0.07 $M_\odot$) dwarfs. These mass estimates are only meant as illustrative values—mass estimates are subject to many uncertainties, and a range of masses and ages will be sampled.

Both the field M8–M9 dwarf and field L dwarf observations show that at a given spectral type, the less massive dwarfs are less active, *even though they are younger*. It is perhaps worth noting that theoretical models suggest that the lower mass objects will be slightly more luminous with a smaller surface gravity (Burrows et al. 1993; Baraffe et al. 1998). The comparison to cluster brown dwarfs is consistent with this trend (Fig. 9). The Pleiades brown dwarfs that have cooled to these ultracool M and L temperatures are less active than old field ultracool M and L dwarfs—but are more active than the low-velocity ultracool M dwarfs. There are thus strong suggestions, as already noted in § 6.1, that activity levels do decrease with age in brown dwarfs and that therefore activity levels are dependent upon tem-

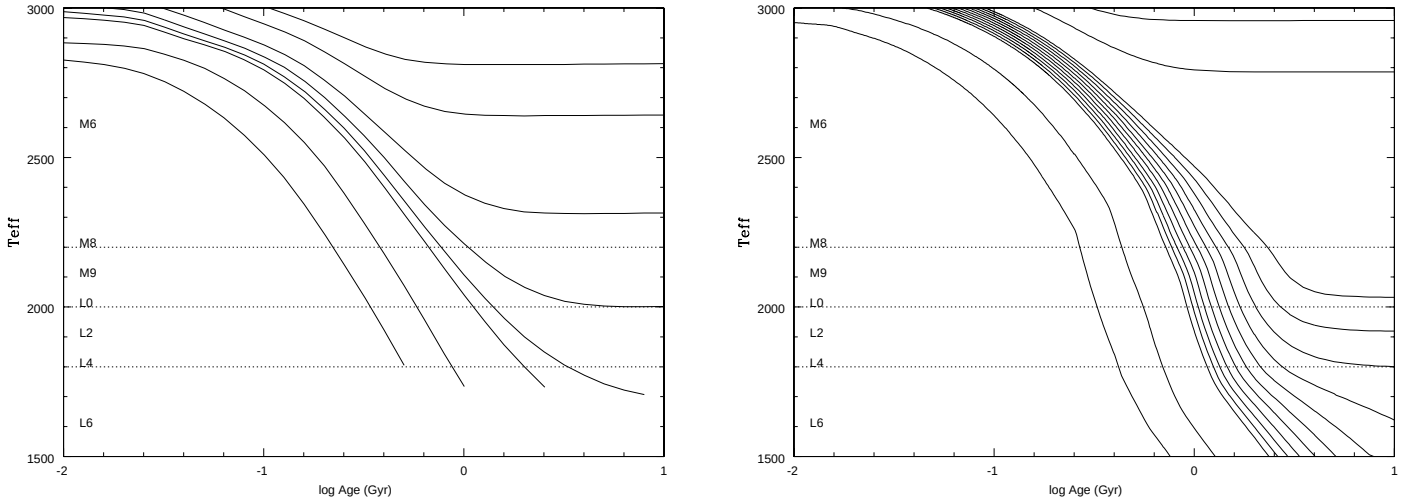

FIG. 10.—Model calculations of brown dwarfs and the lowest mass stars by Baraffe et al. (1998), including preliminary models for lower masses and younger ages (I. Baraffe & G. Chabrier, private communication) and for Burrows et al. (1993, 1997). Along the left-hand axis, the estimated temperature scale of K99 and Reid et al. (1999b) is indicated. The hydrogen-burning limit is 0.072 $M_\odot$ and the lithium-burning limit is 0.055 $M_\odot$ (Chabrier & Baraffe 1997). The models suggest that our spectral range will be populated by stars with age $\gtrsim$ 1 Gyr, transition brown dwarfs burning lithium with 0.4 $\lesssim$ age $\lesssim$ 1 Gyr, and brown dwarfs with lithium with age $\lesssim$ 0.4 Gyr. Both the model temperatures and the spectral-type temperatures are uncertain. These Baraffe et al. models use grainless model atmospheres.

perature, mass, and age. The importance of accretion needs to be investigated for the youngest (<10 Myr) ages. The dominant effect is temperature, as both young and old objects show the rapid fall in activity levels beyond spectral type M7.

At the same time, the models suggest that stars, or at least very long-lived hydrogen-burning transition objects, are likely to exist down to L0–L4 temperatures. This is completely consistent with our empirical finding that the early L dwarfs have old kinematics. We note that Kirkpatrick et al. (1999a) find a temperature of 1900 ± 100 K for the L4 dwarf GD 165B and constrain the age to be greater than 1.2 Gyr using updated models and the white dwarf primary's cooling age and argue it is just below the substellar limit, near the transition region between stars and brown dwarfs (formally, they actually derive the minimum stellar mass using the models). L dwarfs with lithium must be below the lithium-burning limit ($\sim 0.055\ M_\odot$; Chabrier & Baraffe 1997) and younger than 1 Gyr (Fig. 10). The inactivity of these lithium L dwarfs demonstrates that the lowest mass objects cannot sustain significant activity at a temperature (or luminosity) that is adequate for sustaining some activity in older but more massive dwarfs.

The decline in the frequency of activity may be associated with two effects. First, as later spectral types are considered, a larger fraction of very low-mass (substellar) objects contribute, and these are more likely to be inactive in field samples. Second, activity among the L dwarfs may die out in time, since the observed high-velocity L dwarfs are inactive—although we cannot tell if they were ever active. It would be of great interest to find whether or not the early K99/K00 L dwarfs that are active have low or high velocities. The high-velocity, low-activity M9.5 dwarf 2MASSW J0109216+294925 may be a young brown dwarf that happens to have high velocity, an old object that has never been active, or an old stellar M9 dwarf whose chromospheric activity has declined with age. In any case, it is worthy of additional study. We note that the high observed flare rate implies that the rotation rate may decrease with time, even among the "inactive, rapid rotators" if the flaring is associated with mass loss and/or a stellar wind. We speculate this may provide a mechanism for the evolution of activity. Additional observations are needed to determine what the rotational velocities are as a function of mass, spectral type, and age.

What fraction of the ultracool M dwarfs are likely to be substellar? While we cannot identify which individual objects are brown dwarfs, we can identify a number of probably young objects. Three of our M8.0–M9.5 dwarfs show no Hα emission and very low velocity; another three have equally low velocities and $EW_{H\alpha} < 3$ Å. Out of a total population of 32 M8.0–M9.5 dwarfs, our data suggest that 10%–20% are brown dwarfs. These objects should be more likely to have lithium absorption (like LP 944-20), but most of the brown dwarfs will be massive enough to burn lithium. Indeed, we note that none show the distinctive signs of low surface gravity that characterize the Pleiades M8 brown dwarfs Teide 1 and Calar 3 (Martín et al. 1996), so none of our targets are very young ($\sim 10^8$ yr). Approximately 10 objects belong to the low-velocity, low-activity group in the lower left of Figure 8—that is, one-third of the sample, but some fraction of these will stabilize as hydrogen-burning L dwarfs, in order to account for the observed population of high-velocity early L dwarfs. These fractions will be somewhat overestimated for the Galactic disk population, since the old, large-scale height population will be underrepresented locally. Other effects may also be important, such as the fact that we have estimated distances for all dwarfs using one color–absolute magnitude relation. Adding kinematic ages, as in this study, provides an additional constraint on the modeling necessary to determine the field substellar mass function (Reid et al. 1999b).

The nature of the ultracool M dwarfs has been debated for some time in the literature. While conventional wisdom suggested that most if not all field ultracool M dwarfs are stellar, many suggestions that most ultracool M dwarfs are substellar have been made, most of which have been discredited. We remark that Bessell (1991) noted that the ultracool M dwarfs are expected to be a mixture of young brown dwarfs and older stars—and he also noted that there was a paucity of high proper-motion ultracool M dwarfs expected from the stellar population in the LHS catalog (Luyten 1979). Our study has identified a number of high proper-motion M dwarfs that appear on the red POSS plates but were overlooked for the LHS catalog—evidently, the faintest of these targets on the blue plate precluded their detection by Luyten and contributed to the effect noted by Bessell. Our results show that most ultracool M dwarfs are old, and hence stellar, but perhaps 10%–20% are a younger population of brown dwarfs.

We end our discussion with a few caveats due to our photometric selection. Both the relative numbers and kinematics of "active" and "inactive" M dwarfs will be changed if one group is preferentially brighter at M_K for its $J-K$ color. Indeed, the inactive brown dwarf LP 944-20 lies 1 magnitude below the active M dwarf LHS 2397a in the $J-K$, M_K H-R diagram. Preliminary USNO parallaxes show intrinsic dispersion in the H-R diagram for the late M and L dwarfs (C. Dahn, private communication). If inactive ultracool M dwarfs are subluminous compared to our adopted relation, we will have *overestimated* their velocities; correspondingly, if the more active dwarfs are "superluminous," we have underestimated their velocities. Fortunately, this would only strengthen our evidence that active ultracool M dwarfs are older. The intrinsic dispersion presumably depends upon such ill-understood factors as metallicity, age, surface gravity, and dust formation. Another possible bias on activity levels is that we favor the inclusion of unresolved binaries. Among the earlier M dwarfs, very short-period systems have enhanced chromospheric activity owing to tidal effects maintaining high rotation rates (Young, Sadjadi, & Harlan 1987)—however, even if this mechanism works in the ultracool M dwarfs, which seems unlikely if the rotation-activity relation has broken down, only $\sim 5\%$ of earlier type M dwarfs show emission due to this effect, so it should be negligible.

7. SUMMARY

We show that a sample of bright, nearby ultracool M and L dwarfs can be selected without proper-motion bias using 2MASS and PMM scans. Our initial samples include high proper-motion objects, visible on the POSS plates, that should be added to an updated version of the LHS Catalog, and one M8.0 dwarf with a photometric parallax that places it within 10 pc. We intend to continue this study in order to complete the nearby star catalog for the lowest mass stars.

Using our initial sample, we estimate the space density of dwarfs near the hydrogen-burning limit. We show that the

dropoff near the hydrogen-burning limit in the 5 and 8 pc nearby star samples is likely to be due to incompleteness. This is more consistent with a smooth relation across the hydrogen-burning limit. Trigonometric parallaxes and searches for companions will help improve the space density estimate.

Most importantly, we use our spectroscopic observations of our well-defined sample to explore the relationships between age, kinematics, and chromospheric activity for the ultracool M and L dwarfs. We show that the observations can be understood if activity is primarily related to temperature and secondarily mass and age, and that lower mass (substellar) objects have weaker chromospheres. Thus, the classical relation that strong Hα emission implies youth is not valid for these dwarfs. Instead, strong Hα emitters in the field are likely to be old ($\gtrsim$1 Gyr) stars, while weaker emitters are often young ($<$1 Gyr), lower mass brown dwarfs. This does not exclude the idea that for a given dwarf, Hα activity declines with age—but spectral type (temperature) is the observable in the field. The local population of ultracool M dwarfs apparently consists both of the most massive (lithium-burning) brown dwarfs and the lowest mass (hydrogen-burning) stars, with the substellar objects making up a significant fraction of the sample. The early L (L0–L4) dwarfs are consistent with an old, at least partially stellar population. The evidence thus suggests, as do some models, that early L dwarfs can be stable hydrogen-burning stars. Expansion of the sample with follow-up observations should clarify the relative contribution of stars and brown dwarfs to these temperature ranges.

We thank Suzanne Hawley and Mike Skrutskie for useful discussions. We thank the staffs of Las Campanas, Palomar, Keck, and Kitt Peak observatories for their assistance in the observations and the people at University of Massachusetts and IPAC for their efforts in making 2MASS a reality. J. E. G. and J. D. K. acknowledge the support of the Jet Propulsion Laboratory, California Institute of Technology, which is operated under contract with NASA. This work was funded in part by NASA grant AST-9317456 and JPL contract 960847. I. N. R., J. D. K., and J. L. acknowledge funding through a NASA/JPL grant to 2MASS Core Project science This publication makes use of data products from 2MASS, which is a joint project of the University of Massachusetts and IPAC, funded by NASA and NSF. Some of the data presented herein were obtained at the W. M. Keck Observatory, which is operated as a scientific partnership among Caltech, the University of California and NASA. J. E. G. accessed the DSS as a Guest User, Canadian Astronomy Data Centre, which is operated by the Herzberg Institute of Astrophysics, National Research Council of Canada. This research has made use of the SIMBAD database, operated at CDS, Strasbourg, France.

REFERENCES

Basri, G. 1999, American Astronomical Society Meeting 194, 82.08
Basri, G., & Marcy, G. W. 1995, AJ, 109, 762
Baraffe, I., Chabrier, G., Allard, F., & Hauschildt, P. H. 1998, A&A, 337, 403
Bejar, V. J. S., Zapetero Osorio, M. R., & Rebolo, R. 1999, ApJ, 521, 671
Bessell, M. S. 1991, AJ, 101, 662
Bryja, C., Humphreys, R. M., & Jones, T. J. 1994, AJ, 107, 246
Burrows, A., Hubbard, W. B., Saumon, D., & Lunine, J. I. 1993, ApJ, 406, 158
Burrows, A., et al. 1997, ApJ, 491, 856
Bopp, B. W., & Fekel, F. 1977, AJ, 82, 490
Chabrier, G., & Baraffe, I. 1997, A&A, 327, 1039
Delfosse, X., Forveille, T., Perrier, C., & Mayor, M. 1998, A&A, 331, 581
Delfosse, X., Tinney, C. G., Forveille, T., Epchtein, N., Borsenberger, J., Fouque, P., Kimeswenger, S., & Tiphene, D. 1999, A&A, 135, 41
Eggen, O. J. 1993, AJ, 106, 1885
Gizis, J. E., Monet, D. G., Reid, I. N., Kirkpatrick, J. D., & Burgasser, A. J. 2000, MNRAS, 311, 385
Gizis, J. E., & Reid, I. N. 1997, PASP, 109, 849
Gizis, J. E., Reid, I. N., & Monet, D. G. 1999, AJ, 118, 997
Gliese, W., & Jahreiss, H. 1991, Preliminary Version of the Third Catalog of Nearby Stars (pCNS3)
Hawley, S. L., Gizis, J. E., & Reid, I. N. 1996, AJ, 112, 2799 (HGR)
Hawley, S. L., Reid, I. N., & Gizis, J. E. 1999a, in From Giant Planets To Cool Stars, in press
Hawley, S. L., Reid, I. N., & Tourtellot, J. G. 1999b, in the La Palma Conference on Very Low Mass Stars and Brown Dwarfs in Stellar Clusters and Associations, ed. R. Rebolo (Cambridge: Cambridge Univ. Press), in press
Jarrett, T. J., et al. 2000, AJ, 119, 2498
Kirkpatrick, J. D., Allard, F., Bida, T., Zuckerman, B., Becklin, E. E., Chabrier, G., & Baraffe, I. 1999a, ApJ, 519, 834
Kirkpatrick, J. D., Beichman, C. A., & Skruskie, M. F. 1997, ApJ, 476, 311
Kirkpatrick, J. D., Henry, T. J., & McCarthy, D. W. 1991, ApJS, 77, 417
Kirkpatrick, J. D., Henry, T. J., & Simons, D. A. 1995, AJ, 109, 797
Kirkpatrick, J. D., et al. 2000, AJ, in press (K00)
Kirkpatrick, J. D., et al. 1999b, ApJ, 519, 802 (K99)
Kroupa, P., Tout, C. A., & Gilmore, G. F. 1993, MNRAS, 262, 545
Leggett, S. K. 1992, ApJS, 82, 351
Leggett, S. K., Harris, H. C., & Dahn, C. C. 1994, AJ, 108, 944
Liebert, J., Kirkpatrick, J. D., Reid, I. N., & Fisher, M. D. 1999, ApJ, 519, 345
Luhman, K. L., Liebert, J., & Rieke, G. H. 1997, ApJ, 489, L165
Luyten, W. J. 1979, Catalogue of Stars With Proper Motions Exceeding 0".5 Annually (Minneapolis: Univ. of Minnesota) (LHS)
Martín, E. L., Basri, G., Delfosse, X., & Forveille, T. 1997, A&A, 327, L29
Martín, E. L., Basri, G., Gallegos, J. E., Rebolo, R., & Zapatero-Osorio, M. R. 1998a, ApJ, 499, L61
Martín, E. L., Basri, G., & Zapatero-Osorio, M. R. 1999a, AJ, 188, 1005
Martín, E. L., Basri, G., Zapatero-Osorio, M. R., Rebolo, R., & Garcia Lopez, R. J. 1998b, ApJ, 499, L41
Martín, E. L., Delfosse, X., Basri, G., Goldman, B., Forveille, T., & Zapatero-Osorio, M. R. 1999b, AJ, 118, 2466
Martín, E. L., Rebolo, R., & Magazzu, A. 1994, ApJ, 436, 262
Martín, E .L., Rebolo, R., & Zapatero-Osorio, M. R. 1996, ApJ, 469, 706
Monet, D. G., Dahn, C. C., Vrba, F. J., Harris, H. C., Pier, J. R., Luginbuhl, C. B., & Ables, H. D. 1992, AJ, 103, 638
Oke, J. B., et al. 1995, PASP, 107, 375
Perryman, M. A. C., et al. 1997, A&A, 323, L49
Reid, I. N., et al. 1991, PASP, 103, 661
Reid, I. N., & Gizis, J. E. 1997, AJ, 113, 2246
Reid, I. N., Hawley, S. L., & Gizis, J. E. 1995, AJ, 110, 1838
Reid, I. N., Kirkpatrick, J. D., Gizis, J. E., Dahn, C. C., Monet, D. G., Williams, R. J., Liebert, J., & Burgasser, A. 2000, AJ, 119, 369
Reid, I. N., Kirkpatrick, J. D., Gizis, J. E., & Liebert, J. 1999a, ApJ, 527, L105
Reid, I. N., et al. 1999b, ApJ, 521, 613
Schmidt, M. 1968, ApJ, 151, 393
Schneider, D. P., Greenstein, J. L., Schmidt, M., & Gunn, J. E. 1991, AJ, 102, 1180
Stobie, R. S., Ishida, K., & Peacock, J. A. 1989, MNRAS, 238, 709
Tinney, C. G. 1993, AJ, 105, 1169
———. 1996, MNRAS, 281, 644
———. 1998, MNRAS, 296, L42
Tinney, C. G., Mould, J. R., & Reid, I. N. 1993, AJ, 105, 1045
Tinney, C. G., & Reid, I. N. 1998, MNRAS, 301, 1031 (TR)
Tinney, C. G., Reid, I. N., Gizis, J., & Mould, J. R. 1995, AJ, 110, 3014
Wielen, R. 1974, Highlights Astron., 3, 375
Young, A., Sadjadi, S., & Harlan, E. 1987, ApJ, 314, 272
Zapatero-Osorio, M. R., Bejar, V. J. S., Rebolo, R., Martín, E. L., & Basri, G. 1999, ApJ, 524, L115
Zapatero-Osorio, M. R., Rebolo, R., Martín, E. L., Basri, G., Maguzzu, A., Hodgkin, S. T., Jameson, R. F., & Cossburn, M. R. 1997, ApJ, 491, L81